COMMISSARIAT A L'ENERGIE ATOMIQUE

CENTRE D'ETUDES NUCLEAIRES DE SACLAY

Service de Documentation

F91191 GIF SUR YVETTE CEDEX

CEA-CONF - -9488

L3

DOBACZEWSKI J.

CEA Centre d'Etudes Nucléaires de Saclay, 91 - Gif-sur-Yvette (FR). Inst. de Recherche Fondamentale (IRF)

NUCLEAR DEFORMATION: A PROTON-NEUTRON EFFECT

Communication présentée à : International Conference on Contemporary Topics in Nuclear Structure Physics

Cocoyoc (MX)
9-11 Jun 1988

Invited talk presented at Int. Conf. on Contemporary Topics in Nuclear Structure Physics, Cocoyoc June 9-14,1988.

NUCLEAR DEFORMATION: A PROTON-NEUTRON EFFECT?

Jacek Dobaczewski[1]

Service de Physique Théorique, CEN Saclay, 91191 Gif-sur-Yvette Cedex, France

ABSTRACT

The Hartree-Fock plus BCS method with the Skyrme interaction is used to analyse the equilibrium deformations of nuclei in the A≃100 region. It is shown that the theoretical results are consistent with the N_nN_p classification scheme. Relations between the nuclear deformation effects and the neutron-proton interaction are discussed.

1. INTRODUCTION

The concept of nuclear deformation is a very useful and efficient tool to analyze various properties of non-magic nuclei. It is by now well understood in terms of the spontaneous symmetry breaking mechanism and in terms of the nuclear shell structure. From the single-particle spectrum of particles moving in a deformed mean potential, one can immediately deduce the magnitude of deformation effects in a given region of the nuclear chart. The guiding rule is that the Fermi energy 'avoids' the regions of the large single-particle level density. Such a rule has deep roots in the general properties of many-fermion systems and has successfully been employed in e.g. the shell correction method.

The single-particle spectrum of a nucleus is determined by the nuclear two-body interactions, and hence the roots of the nuclear deformation effects can also be looked for in the properties of nuclear forces. Within the nuclear shell model the long-range neutron-proton (n-p) interaction has been assumed[1-3] to be a source of

[1] Permanent address: Institute of Theoretical Physics, Warsaw University, Hoża 69, PL-00681 Warsaw, Poland.

Invited talk presented at Int. Conf. on Contemporary Topics in Nuclear-Structure Physics, Cocoyoc, Mexique June 9-14, 1988

Saclay, Ph-T/88/122

the nuclear deformation. On the other hand, the *isoscalar* long-range quadrupole-quadrupole (Q-Q) interaction has been used in the Pairing-plus-Quadrupole model (see e.g. Ref. 4), where the neutron-proton effects are implicitly introduced by assuming equal deformations for protons and neutrons. Both suppositions can be quantitatively reconciled[5], and the relations between the isoscalar and the isovector Q-Q coupling constants clearly show that the n-p component dominates the Q-Q interaction.

A method to analyze the properties of the two-body effective interaction with respect to the nuclear deformability has recently been formulated in Ref. 5. It has been shown there that the Skyrme force SIII[6] contains the correct Q-Q component, and the effects of the n-p interaction on the nuclear deformation have been analyzed on the example of the germanium isotopes. In the present paper, the same method is used to study the deformation properties of nuclei from the A≃100 region.

Experimental data for low-lying collective quadrupole states have recently been discussed by Casten[7,8] in terms of a simple N_nN_p parametrization by the product of numbers of active valence protons and neutrons. The importance of the N_nN_p parameter for a description of the experimental data is often considered as a strong argument supporting the dominant role of the n-p interaction. The main goal of the present study is to unveil the existence of the N_nN_p systematics in the theoretical results of the Hartree-Fock method, and to analyze its relation to the n-p component of the effecive interaction.

2. HARTREE-FOCK CALCULATIONS IN THE A≃100 REGION

The Skyrme force[9], which we use in this study, consists of several terms, of which the simplest one is the ordinary contact force,

$$V_{12} = t_0\delta(r_1 - r_2)(1 - x_0P_\sigma) \quad , \tag{1}$$

where $P_\sigma = \frac{1}{2}(1 + \sigma_1\cdot\sigma_2)$ is the operator exchanging spin quantum numbers of the two interacting nucleons, and t_0 and x_0 are the parameters. The isospin dependence is hidden in the antisymmetrizing operator $(1 - P_\sigma P_\tau P_M)$, by which the V_{12} intreraction is multiplied. The operator $P_\tau = \frac{1}{2}(1 + \tau_1\cdot\tau_2)$ and the Majorana operator P_M exchange the isospin and the spatial coordinates, respectively. Because of the presence of the antisymmetrizing operator, one has

$$\delta(r_1 - r_2)(1 - x_0P_\sigma) = \delta(r_1 - r_2)(1 + x_0P_\tau) \quad , \tag{2}$$

which results from the fact that the P_M operator is equal to unity when multiplied by $\delta(r_1 - r_2)$. Hence the Skyrme force can be considered as being explicitly dependent on spin or isospin, but in fact, because of the antisymmetrization, it depends on both of them.

Apart from the pure contact component, the Skyrme force SIII contains the terms in which $\delta(r_1 - r_2)$ is multiplied by $(\nabla_1^2 + \nabla_2^2)$, $\nabla_1 \cdot \nabla_2$ or $\rho(r)$, and it also contains the two-body spin-orbit force. Altogether it depends on 6 parameters, which have been adjusted to reproduce some bulk properties of nuclei, and in particular, the volume and surface energy, the symmetry energy, the Fermi momentum, the effective mass, and the spin-orbit splitting of the single-particle states.

The isospin dependence of the Skyrme force is thus determined by the adjustment to the symmetry energy. The fitting has been is done[6] by referring only to the magic nuclei, and the capability of the force to describe the deformation effects has not been taken into consideration. Despite of that, the Skyrme force has been successfully used to describe deformed nuclei.[10-12]

In the present study, the deformation properties of the even-even nuclei with $38 \leq Z \leq 48$ and $50 \leq N \leq 72$ are determined by the Hartree-Fock plus BCS (HF+BCS) method. The HF equations were solved by expanding the single-particle wave functions in the spherical harmonic oscillator basis extending up to the $N_0 = 14$ major shell. For every nucleus in the specified range, we have performed unconstrained calculations on the oblate and on the prolate deformation side, which has determined the positions of the minima. In addition, the constrained calculations at the spherical extremum (Q=0) has also been done. For those nuclei, where the deformed minima do not exist, the unconstrained calculations converge towards the unique spherical solution.

The pairing correlations have been taken into account by the BCS method and by assuming the fixed pairing gap parameters[10] determined from the odd-even experimental mass differences.[13] In nuclei where the experimental values are not accessible, we have used the values of the pairing gap from the closest isotope where they are known.

In Fig. 1a the prolate equilibrium deformations, i.e. the values of the mass quadrupole moment Q^{eq} for which the HF+BCS energy has the minimum, are presented. In Fig. 1b the equilibrium deformation energies $\delta E^{eq} = E(Q^{eq}) - E(Q=0)$ corresponding to the prolate equilibrium deformations are shown. It can be seen that the equilibrium deformations of the nuclei from the A$\simeq$100 region increase

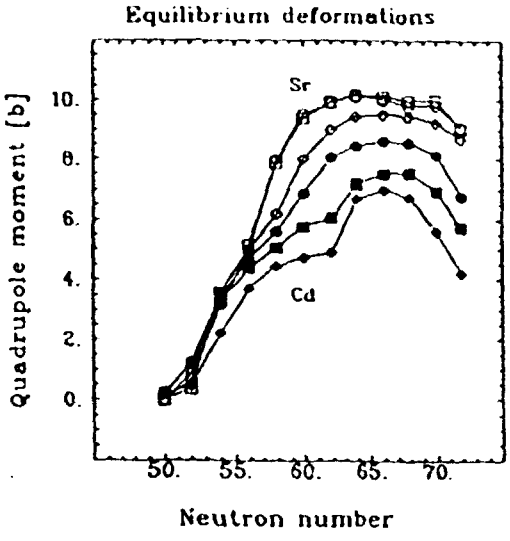

Fig. 1a: Prolate equilibrium deformations Q^{eq} of nuclei in the A≃100 region plotted as a function of neutron number. The mass quadrupole moments are expressed in barns.

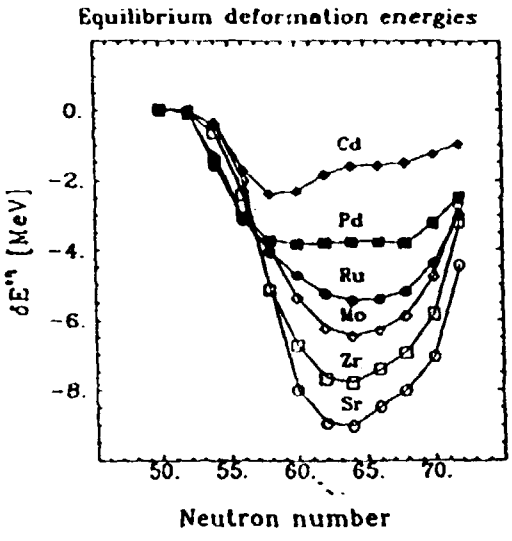

Fig. 1b: Prolate equilibrium deformation energies $\delta E^{eq}=E(Q^{eq})-E(Q=0)$ of nuclei in the A≃100 region plotted as a function of neutron number.

with increasing neutron number N and decrease with increasing proton number Z. This is consistent with the fact that, with increasing N, the nuclei in this region get further apart from the neutron magic number N=50, and with increasing Z they get closer to the proton magic number Z=50. This simple pattern is disturbed for nuclei with $N < 60$, which can be seen in the results shown in Figs. 2a and 2b, where the same data are plotted as functions of the proton number Z. For $N \geq 60$, the equilibrium deformation energies are monotonic functions of Z, while for $N < 60$ both Q^{eq} and δE^{eq} show extrema or an irregular behaviour.

The qualitative change in structure occuring at N=60, predicted by the HF+BCS calculations, is in agreement with the analysis of the experimental data performed by Casten,[8] who classified the energies and the B(E2) transition rates of the low-lying collective states according to the number of active valence neutron and proton holes or particles, N_n and N_p, respectively. It has been shown, that for $N < 60$ one should consider as being active the protons which are in the shell between Z=38 and Z=50, while for $N \geq 60$, those which are between Z=28 and Z=50. With the numbers N_n and N_p calculated according to such a prescription, the experimental data have been shown to depend smoothly on the product N_nN_p .

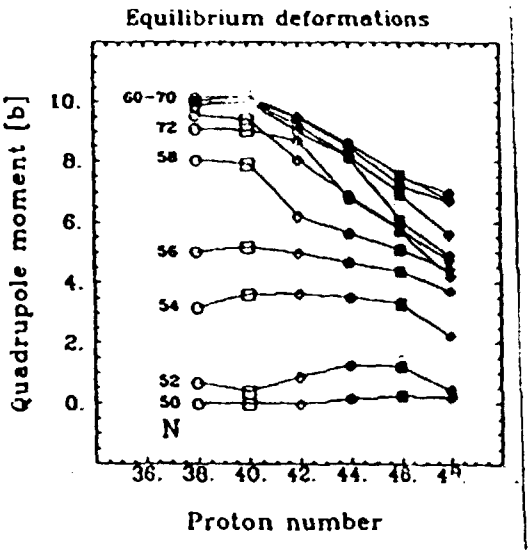

Fig. 2a: Same as in Fig. 1a plotted as a function of proton number.

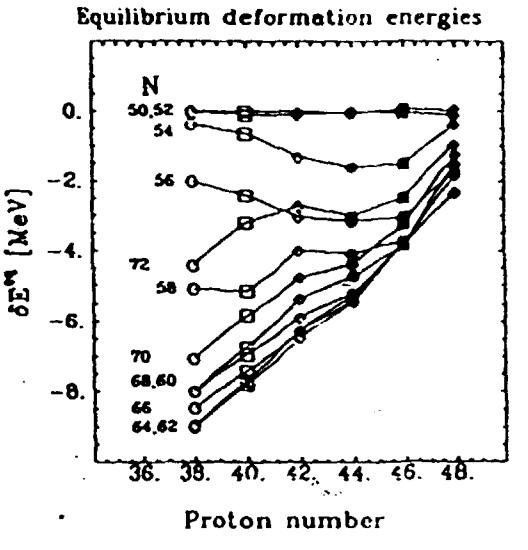

Fig. 2b: Same as in Fig. 1b plotted as function of proton number.

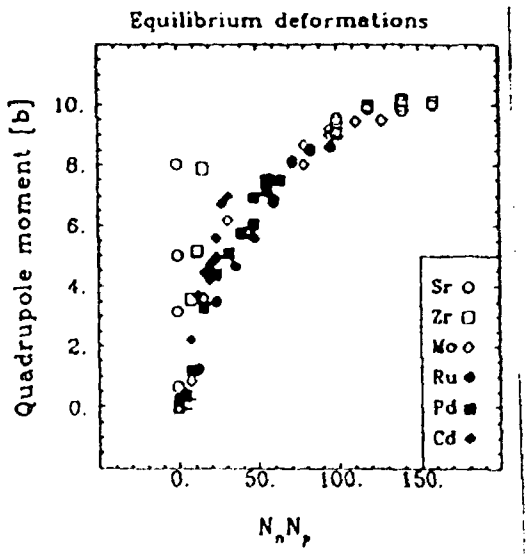

Fig. 3a: Same as in Fig. 1a plotted as a function of N_nN_p .

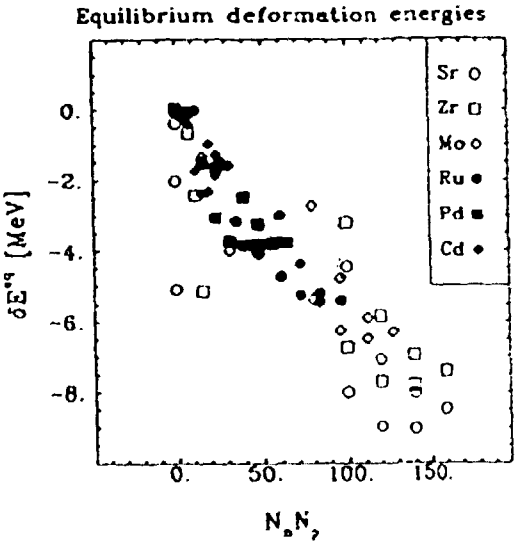

Fig. 3b: Same as in Fig. 1b plotted as a function of N_nN_p .

In Figs. 3a and 3b we plot our results as functions of the product N_nN_p . One can see a striking unification of the theoretical results when thay are presented in this way (see also Ref. 14). Especially the equilibrium deformations tend to cluster around a smooth curve, while the equilibrium deformation energies lie in a well defined band. Departures from the regular behaviour are seen for the Sr

and Zr isotopes with N=58, for which the consideration of the shell $38 \leq Z \leq 50$ seems not to be justified. In the plot of the equilibrium deformation energies, the points are rather scattered at large N_nN_p , which can be attributed to two facts: (i) the equilibrium deformation energies have clear extrema at N=64, and not exactly at the middle of the neutron the shell, i.e. at N=66, and (ii) the heavy Sr isotopes have larger equilibrium deformation energies then the heavy Zr isotopes, which suggests that the number of active protons (proton holes) should be N_p=12 and N_p=10 for Sr and Zr isotopes, respectively (and not N_p=10 for both these clements, as resulting from the proton shell $28 \leq Z \leq 50$). On the other hand, the results for the equilibrium deformations support the standard way of determining the number of active particles. This inconsistency illustrates the extent to which the HF+BCS results can actually be classified according to the N_nN_p scheme.

3. THE N=56 SUBSHELL CLOSURE

Before discussing the hypothetical relation between the N_nN_p unification scheme and the dominance of the n-p component in the nuclear interaction, let us analyze the source of the change in structure occuring at N=60. Federman and Pittel[3] have proposed a suggestive interpretation of such a change. In their picture, both the $1g_{7/2}$ neutron and the $1g_{9/2}$ proton orbitals are fairly empty for $N < 60$, and thus the effect of the n-p interaction is small, (interaction is strongest for nucleons occupying large-j orbitals[1]). When the neutrons start to occupy the $1g_{7/2}$ orbital, they pull the protons into the $1g_{9/2}$ subshell, and by the mutual interaction and polarization both spin-orbit partners become occupied, which results in a brusque onset of deformation.

The mechanism proposed by Federman and Pittel invokes two different effects,[15] which can lead to changes of the occupation probabilities of the large-j orbitals with increasing neutron number: (i) the *monopole* effect which shifts the positions of the spherical single-particle orbits, and (ii) the *quadrupole* effect which is responsible for the polarization of the 0^+ pairs and the configuration mixing. In our approach the occupation probabilities are determined by the BCS method, and therefore they depend only on the single-particle energies and on the pairing gaps. In Fig. 4a the spherical-shape neutron and proton occupation probabilities as functions of neutron number are presented for the series of strontium isotopes. The results show that the occupation probability of the $1g_{9/2}$ proton state, as well as other proton orbitals, is practically constant in the studied range of neutron numbers. It means that the Federman and Pittel n-p monopole mechanism is not

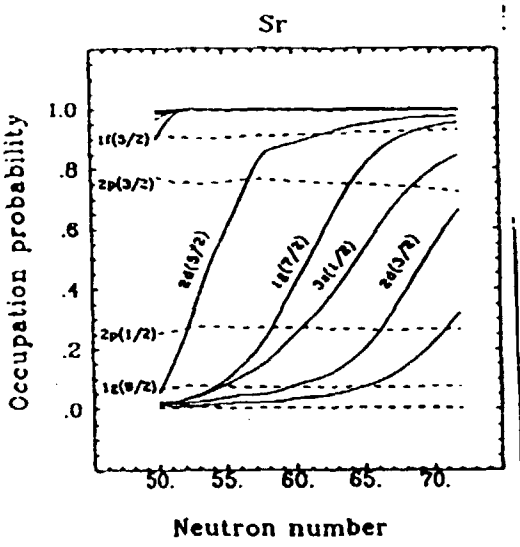

Fig. 4a: Occupation probabilities of spherical single-particle neutron (solid lines) and proton (dashed lines) states in the strontium isotopes.

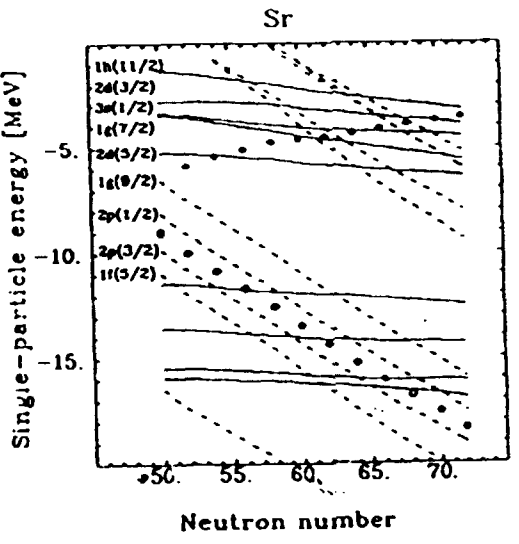

Fig. 4b: Spherical single-particle neutron (solid lines) and proton (dashed lines) levels in the strontium isotopes. The neutron and proton Fermi energies are shown by the closed and open circles, respectively.

present in our Hartree-Fock calculations, and the presence of the $1g_{7/2}$ neutrons does not increase the $1g_{9/2}$ occupation probability. This is clearly related to the fact that the position of the $1g_{9/2}$ proton orbital relative to the Fermi energy is in our calculations *not* affected by the presence of the $1g_{7/2}$ neutrons (Fig. 4b). The same conclusion can be drawn for the palladium isotopes, Figs. 5a and 5b. Despite of the absence of the Federman and Pittel monopole effect, the change in structure at N=60 is visible in our results, and requires another explanation.

In terms of the spherical shell model, an explanation can be found by observing that the single-particle energy of the $1g_{7/2}$ neutron orbital depends significantly on both neutron and proton number (Figs. 4b and 5b). A necessity of the relative changes of this energy has already been suggested from an analysis of experimental data.[16] In the light strontium isotopes, the $1g_{7/2}$ state lies rather high in energy, leaving the $2d_{5/2}$ neutron state well separated from the rest of the shell. The $2d_{5/2}$ orbital does not have large enough quadrupole moment to create the deformation by itself, and consequently the nuclei with $N < 58$ stay nearly spherical. When the neutron Fermi energy enters the $1g_{7/2}$ subshell, the nuclear deformation sets in. This effect disappears at larger proton numbers, where the energy of the $1g_{7/2}$

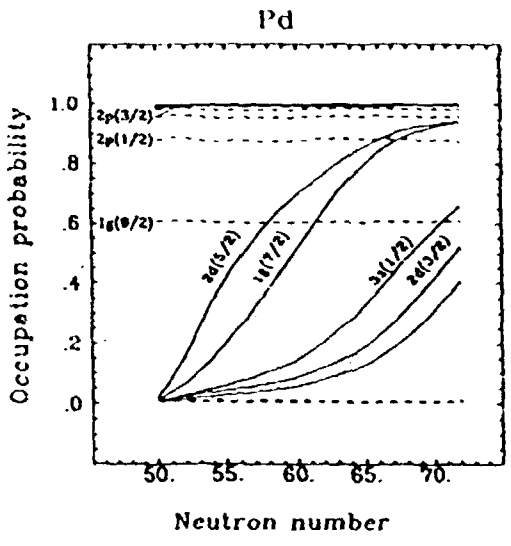

Fig. 5a: Same as in Fig. 4a but for the palladium isotopes.

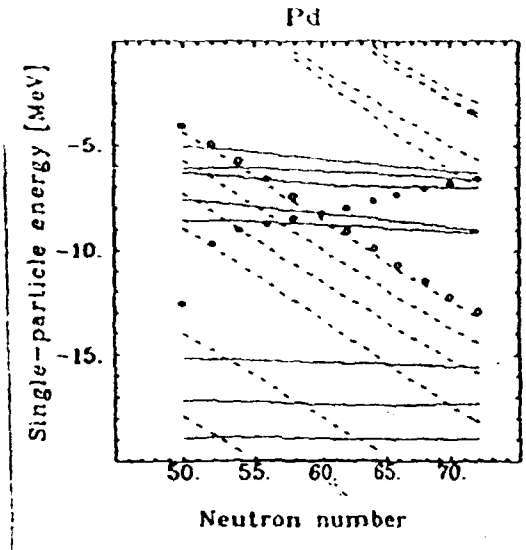

Fig. 5b: Same as in Fig. 4b but for the palladium isotopes.

neutron orbital is smaller (Fig. 5b) and the spherical gap at N=56 closes up, and where the proton N=38, 40 gaps do not stabilize the sherical shape.[17]

With increasing deformation the quadrupole Federman and Pittel effect becomes more and more important. However, based on the occupation probabilities calculated for the deformed orbitals[18], and on the deformed shell-model analysis of the intruder states,[19] one can attribute the increase of deformation mainly to the dominant role played by the $1h_{11/2}$ neutron orbital, and less to that of the $1g_{7/2}$ subshell.

Our results show that the proton spherical gap at Z=38 (Figs. 4b and 5b) is not affected by the number of neutrons. Therefore, the different way of counting the active protons below and above N=60 may in fact be an effective way to account for the neutron subshell closure, which in our case is visible at N=56. It is, however, still possible that the changes in the position of the $1g_{7/2}$ neutron orbital are caused by the presence of the strong n-p interaction; the influence of a varying one-body spin-orbit intensity can be an alternative explanation.

The details of the subshell structure can be different for various Skyrme forces (cf. Ref. 12), and the effects of the N=56 gap can thus be different. For the SIII force, these effects are rather weak and only visible when comparing results for many nuclei.

4. NEUTRON-PROTON INTERACTION ENERGIES

In the HF approach one can explicitly calculate the n-n, p-p and n-p interaction energies as

$$E^{\tau\tau'} = \frac{1}{1+\delta_{\tau\tau'}} \mathrm{Tr}_1 \mathrm{Tr}_2 \rho_1^{\tau} V_{12}^{\tau\tau'} \rho_2^{\tau'} \quad , \tag{3}$$

where $\tau, \tau' =$p or n, $V_{12}^{\tau\tau'}$ are the isospin components of the Skyrme interaction, and ρ^n and ρ^p are the neutron and proton one-body density matrices determined by the HF+BCS method.

The nuclear ground state energy E is composed of five terms:

$$E = E^{kin} + E^{pair} + E^{nn} + E^{pp} + E^{np} \quad , \tag{4}$$

where E^{kin} and E^{pair} are the kinetic and the pairing energy, respectively. The Coulomb energy is included in the p-p interaction energy E^{pp}. The dependence of E and its five constituents on neutron number is shown in Fig. 6 for the spherical shapes of the molybdenum isotopes. The pairing energy and the p-p energy (in which the Coulomb energy strongly cancels the nuclear component) contribute much less to the binding energy then the three other components. The n-p interaction energy E^{np} is several times stronger then the n-n energy E^{nn}. Consequently, the nuclear binding is a result of cancelation between negative sum $E^{np} + E^{nn}$ and the positive kinetic energy E^{kin}. These results indicate that the n-p interaction is indeed the most important factor in providing for the nuclear binding.

On the top of large values of E^{np}, E^{nn}, and E^{kin}, one is not able to see shell effects, which are smaller by around three orders of magnitude. In order to make the shell effects visible, the deformation energy δE=E-$E(Q$=0), together with its five components,

$$\delta E = \delta E^{kin} + \delta E^{pair} + \delta E^{nn} + \delta E^{pp} + \delta E^{np} \quad , \tag{5}$$

is presented in Figs. 7a and 7b. In the spherical nucleus ^{92}Mo (Fig. 7a), the increase of the energy with increasing $|Q|$ is due to the increase of δE^{np} and δE^{nn}, which is partly compensated by the decrease of δE^{kin} and δE^{pp}. The situation is almost opposite in ^{106}Mo, where the decrease of δE is a result of the decrease of all interaction energies, δE^{nn}, δE^{pp}, and δE^{np}, partly balanced by a strong increse of δE^{kin}. On should note, that in both cases the *explicite* role of the pairing energy is negligible, and the pairing correlations influence the deformation properties only through the other components of δE.

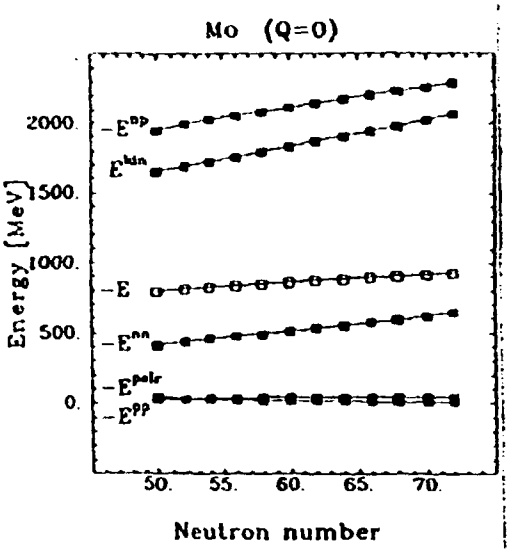

Fig. 6: Spherical ground-state energies of the molybdenum isotopes, and their five constituents (as given by Eq. (4)) presented as a function of neutron number.

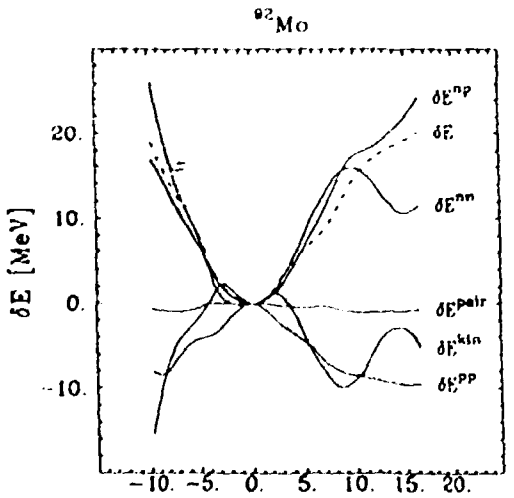

Fig. 7a: Variation of the ground-state energy δE and its five constituents (as presented in Eq. (5)) with the quadrupole moment for ^{92}Mo.

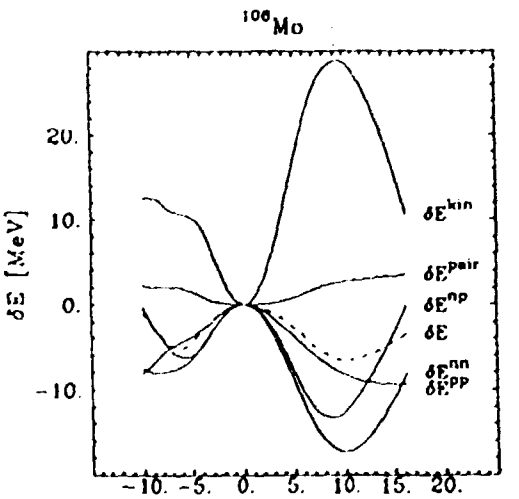

Fig. 7b: Same as in Fig. 7a but for ^{106}Mo.

The results shown in Figs. 7a and 7b seem to negate the dominant role of the n-p interaction in constituting the deformation energy. The effect of δE^{np} is apparently equally large. But a crucial influence of the kinetic energy suggests that the splitting of E into the five components given by Eqs. (4) and (5) may not necessarily be the best way of looking at the n-p effects. The influence of the interaction is, of course, present in E^{kin}, because the nuclear wave function for which the mean value of the kinetic energy operator is calculated, is determined within the variational method where the interactions are essential. Hence, the decomposition of the energy, as given by Eqs. (4) and (5), is not very instructive when studying effects of the interactions on nuclear deformation.

Another way of analyzing the deformation energy δE consists in expanding every isospin component of the interaction energy as[5)]

$$E^{\tau\tau'} = E_0^{\tau\tau'} + E_2^{\tau\tau'} + E_4^{\tau\tau'} + \dots \quad , \tag{6}$$

where the $J = 0, 2, 4, \dots$ terms can be interpreted[20)] as the monopole interaction energy and the quadrupole, hexadecapole, etc., correlation energies. The multipole terms are defined as

$$E_J^{\tau\tau'} = \frac{1}{1+\delta_{\tau\tau'}} \mathrm{Tr}(\mathrm{Tr} V \rho^{\tau}) \rho_J^{\tau'} \quad , \tag{7}$$

where ρ_J^{τ} is the rank-J spherical operator obtained by the multipole decomposition of the density matrix,

$$\rho^{\tau} = \rho_0^{\tau} + \rho_2^{\tau} + \rho_4^{\tau} + \dots \tag{8}$$

In terms of the multipole components, the ground state energy can be presented as

$$E = E_0 + E_2 + E_4 + \dots \quad , \tag{9}$$

where the monopole part E_0 reads

$$E_0 = E^{kin} + E^{pair} + E_0^{nn} + E_0^{pp} + E_0^{np} \quad , \tag{10}$$

while the quadrupole, hexadecapole, etc., energy is the sum of different isospin components:

$$E_2 = E_2^{nn} + E_2^{pp} + E_2^{np} \quad . \tag{11}$$

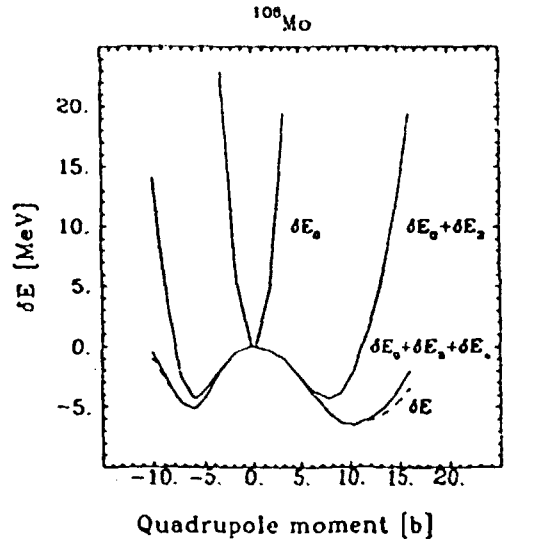

Fig. 8: Deformation energy δE=E-$E(Q$=0) of ^{106}Mo (dashed line), its monopole part δE_0 alone and corrected by the quadrupole δE_2 and the hexadecapole δE_4 correlation energies.

In Fig. 8 we present the deformation energy of ^{106}Mo together with the corresponding monopole component δE_0 and the consequtive sums $\delta E_0 + \delta E_2$ and $\delta E_0 + \delta E_2 + \delta E_4$. As seen in the results shown in Fig. 8, the positive monopole energy δE_0 is very different from δE and rapidly increases with $|Q|$. The quadrupole component δE_2 is negative and brings δE_0 down almost to δE, while the addition of δE_4 exhausts δE almost completely. The deformation energy is thus composed of the monopole term balanced by the quadrupole term, and a relatively small hexadecapole correction. Neglecting this correction for the subsequent analysis, and noting that the spherical symmetry imposes the vanishing of the multipole correlation energies at Q=0, i.e. $\delta E_2 = E_2$, we have

$$\delta E = \delta E_0 + E_2^{nn} + E_2^{pp} + E_2^{np} \quad . \tag{12}$$

All four terms are nearly quadratic functions of the quadrupole moment, which justifies the determination of the quadrupole-quadrupole (Q-Q) coupling constants as[5]

$$\kappa_{\tau\tau'} = (1+\delta_{\tau\tau'})\frac{E_2^{\tau\tau'}}{Q_\tau Q_{\tau'}} \quad , \tag{13}$$

from which the isoscalar and isovector, κ_0 and κ_1, coupling constants can be calculated:

$$\kappa_0 = \frac{1}{4}(\kappa_{nn}+\kappa_{pp}) + \frac{1}{2}\kappa_{np} \quad , \tag{14}$$

$$\kappa_1 = \frac{1}{4}(\kappa_{nn}+\kappa_{pp}) - \frac{1}{2}\kappa_{np} \quad . \tag{15}$$

For all the nuclei studied here, we have performed additional constrained HF+BCS calculations requiring the quadrupole moment to be equal to $-1.5b$, and from these results we have determined the coupling constants κ_0 and κ_1, which are plotted in Fig. 9a as functions of mass number. In the same Figure, we show the estimates[21,22,5] $\kappa_0 = -23.3A^{-7/3}MeV\,fm^{-4}$ and $\kappa_1 = 15.4A^{-7/3}MeV\,fm^{-4}$ resulting from the harmonic-oscillator model. The derived Q-Q coupling constants agree very well with the simple estimates, which are consistent with the experimental data for giant quadrupole resonances, suggesting that the correct Q-Q component is contained in the Skyrme interaction. The ratio of the calculated isovector and isoscalar coupling constants is almost mass independent and reads

$$\kappa_1/\kappa_0 \simeq -0.5 \quad , \tag{16}$$

which results in the ratio of the n-p to the n-n and p-p coupling constants $\kappa_{np}/\kappa_{nn} = \kappa_{np}/\kappa_{pp} \simeq 3$, and illustrates the dominance of the n-p component in the nuclear Q-Q interaction.

The contribution of the isoscalar and isovector Q-Q interaction to the deformation energy is of the order of $\kappa_0(Q_n+Q_p)^2$ and $\kappa_1(Q_n-Q_p)^2$, respectively. Since in the low-energy quadrupole mode one has $Q_n \simeq Q_p$, the isovector contribution is small compared to the isoscalar one. Therefore, the deformation energy results from a cancelation between the positive monopole energy, and the negative quadrupole isoscalar energy. The cancelation can be illustrated by introducing the monopole stiffness paramater C_0,

$$C_0 = 2\frac{\delta E_0}{Q\,Q} \quad , \tag{17}$$

which has been calculated from the HF+BCS results constrained at Q=1.5b. Figure 9b shows the values of C_0 in the A$\simeq$100 region. On the top of smooth depen-

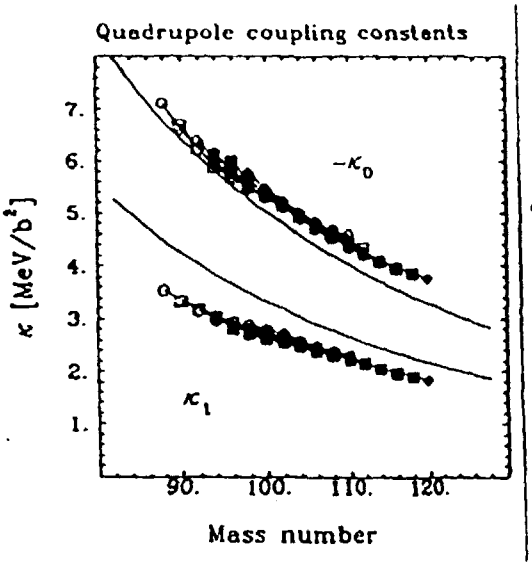

Fig. 9a: Isoscalar κ_0 and isovector κ_1 quadrupole coupling constants derived from the Hartree-Fock results, Eqs. (13) - (15), compared to the estimates from the harmonic-oscillator model (solid lines) for A≃100 nuclei.

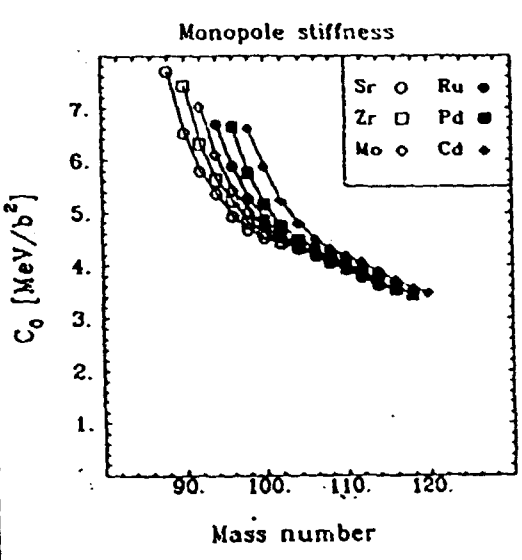

Fig. 9b: Monopole stiffness parameter C_0, Eq. (17), as a function of mass number.

dence of C_0 on mass number, one can see the influence of the N=50 closed shell. The sum of κ_0 and C_0 is much smaller than each of these, and reflects deformation changes in the nuclei studied. Because the shell structure influences the values of C_0 much stronger than those of κ_0, one can say that C_0 is the main factor in deciding which nucleus is spherical, and which is the deformed one. The monopole energy can be related to the mean value of the *spherical* mean field Hamiltonian calculated for a deformed state. Mixing of the spherical configurations, which occurs in the deformed state, and which is favoured by the Q-Q interaction, is unfavoured with respect to the spherical field. The deformation results from such two opposite tendencies. Depending on the position of the Fermi energy in the spherical shell, the monopole effect is stronger or weaker, and as a result some nuclei are spherical ond other are deformed. On the other hand, the Q-Q intreraction energies (as shown by the values of κ_0) are much less shell-dependent, and provide for a steady deformation-driving factor. In this way, the mean value of the Q-Q interaction (in which the Q_n-Q_p component is the dominant one) *in the equilibrium point* is correlated with the product N_nN_p , while the position of the equilibrium point itself is decided by the monopole energy.

5. CONCLUSIONS

In summary, the following conclusions can be drawn from our HF+BCS analysis of the A$\simeq$100 nuclei:

- Equilibrium deformations and equilibrium deformation energies obtained in terms of the HF+BCS method with the Skyrme interaction can be systematized by considering the product $N_n N_p$ as a useful paramater unifying the results for various nuclei in the A$\simeq$100 region.

- Theoreticaly, one does not find any obvious indication for the monopole influence of the $1g_{7/2}$ neutrons on the $1g_{9/2}$ protons. The structure of the proton spherical single-particle spectrum does not seem to be depenent on the number of neutrons.

- A change in structure at N=60 is predicted theoreticaly for different elements. One can interprete this change in terms of the position of the $1g_{7/2}$ neutron orbital with respect to other states of the $50 \leq N \leq 82$ shell.

- A dominant role of the n-p quadrupole component of the Skyrme interaction in generating the nuclear deformation is found. However, this component depends weakly on the shell structure Whether a given nucleus is spherical or deformed depends on how strongly the monopole energy resists the steady quadrupole interaction.

This work was supported in part by the Polish Ministry of National Education under Contract CPBP 01.09.

REFERENCES

1. de Shalit, A. and Goldhaber, M., *Phys. Rev.* **92**, 1211 (1953).
2. Talmi, I., *Rev. Mod. Phys.* **34**, 704 (1962).
3. Federman, P. and Pittel, S., *Phys. Rev.* **C20**, 820 (1979).
4. Bès, D.R. and Sorensen, R.A., *Adv. Nucl. Phys.* **2**, 129 (1969).
5. Dobaczewski, J., Nazarewicz, W., Skalski, J. and Werner, T., *Phys. Rev. Lett.* **60**, 2254 (1988).
6. Beiner, M., Flocard, H., Van Giai, N. and Quentin, P., *Nucl. Phys.* **A238**, 29 (1975).
7. Casten, R.F., *Phys. Lett.* **152B**, 145 (1985).

8. Casten, R.F., *Nucl. Phys.* **A443**, 1 (1985).

9. Vautherin, D. and Brink, D.M., *Phys. Rev.* **C5**, 626 (1972).

10. Vautherin, D., *Phys. Rev.* **C7**, 296 (1973).

11. Flocard, H., Quentin, P., Kerman, A.K. and Vautherin, D., *Nucl. Phys.* **A203**, 433 (1973).

12. Bonche, P., Flocard, H., Heenen, P.H., Krieger, S.J. and Weiss, M.S., *Nucl. Phys.* **A443**, 39 (1985).

13. Wapstra, A.H. and Audi, G., *Nucl. Phys.* **A432**, 1 (1985).

14. Casten, R.F., von Brentano, P., Gelberg, A. and Harter, H., *Journ. of Phys.* **G12**, 711 (1986).

15. Hyde, K., Van Isacker, P., Casten, R.F. and Wood, J.L., *Phys. Lett.* **155B**, 303 (1985).

16. Mach, H., *Selected Topics in Nuclear Structure*, Proceedings of the Twenty-third Zakopane School on Physics, (Institute of Nuclear Physics, Kraków, 1988).

17. Nasarewics, W. and Werner T., Proceedings of the International Workshop on Nuclear Structure of the Zirconium Region, Bad Honnef, April 1988.

18. Pfeiffer, B. and Kratz, K.-L., Proceedings of the International Workshop on Nuclear Structure of the Zirconium Region, Bad Honnef, April 1988.

19. Nasarewicz, W., *in these proceedings.*

20. Dobaczewski, J. and Skalski J., to be published.

21. Bohr, A. and Mottelson, B., "Nuclear Structure" (Benjamin, New York, 1975), Vol 2.

22. Bès, D.R., Broglia, R.A. and Nilsson, B.S., *Phys. Rep.* **16C**, 1 (1975).